

1 *BIRC6* modifies risk of invasive 2 bacterial infection in Kenyan 3 children.

4 James J Gilchrist^{1,2,3*}, Silvia Kariuki⁴, James A Watson^{5,6}, Gavin Band³, Sophie
5 Uyoga⁴, Carolyn M Ndila⁴, Neema Mturi⁴, Salim Mwarumba⁴, Shebe
6 Mohammed⁴, Moses Mosobo⁴, Kirk A Rockett³, Alexander J Mentzer³, Dominic P
7 Kwiatkowski^{3,7}, Adrian VS Hill^{3,8}, Kathryn Maitland^{4,9}, J Anthony G Scott^{4,10},
8 Thomas N Williams^{4,11*}

***For correspondence:**

james.gilchrist@paediatrics.ox.ac.uk (JJG);
twilliams@kemri-wellcome.org
(TNW)

9 ¹Department of Paediatrics, University of Oxford, Oxford, UK; ²MRC-Weatherall
10 Institute of Molecular Medicine, University of Oxford, Oxford, UK; ³Wellcome Centre for
11 Human Genetics, University of Oxford, Oxford, UK; ⁴KEMRI-Wellcome Trust Research
12 Programme, Centre for Geographic Medicine Research-Coast, Kilifi 80108, Kenya;
13 ⁵Centre for Tropical Medicine and Global Health, Nuffield Department of Medicine,
14 University of Oxford, Oxford, UK; ⁶Mahidol Oxford Tropical Medicine Research Unit,
15 Faculty of Tropical Medicine, Mahidol University, Bangkok, Thailand; ⁷Wellcome Sanger
16 Institute, Cambridge, UK; ⁸The Jenner Institute, University of Oxford, Oxford, UK;
17 ⁹Division of Medicine, Imperial College, London, UK; ¹⁰Department of Infectious
18 Disease Epidemiology, London School of Hygiene & Tropical Medicine, London, UK;
19 ¹¹Institute for Global Health Innovation, Department of Surgery and Cancer, Imperial
20 College, London, UK

22 Abstract

23 Invasive bacterial disease is a major cause of morbidity and mortality in African children. Despite
24 being caused by diverse pathogens, children with sepsis are clinically indistinguishable from one
25 another. In spite of this, most genetic susceptibility loci for invasive infection that have been
26 discovered to date are pathogen specific and are not therefore suggestive of a shared genetic
27 architecture of bacterial sepsis. Here we utilise probabilistic diagnostic models to identify
28 children with a high probability of invasive bacterial disease among critically unwell Kenyan
29 children with *P. falciparum* parasitaemia. We construct a joint dataset including 1,445
30 bacteraemia cases and 1,143 severe malaria cases, and population controls, among critically
31 unwell Kenyan children that have previously been genotyped for human genetic variation. Using
32 these data we perform a cross-trait genome-wide association study of invasive bacterial infection,
33 weighting cases according to their probability of bacterial disease. In doing so we identify and
34 validate a novel risk locus for invasive infection secondary to multiple bacterial pathogens, that
35 has no apparent effect on malaria risk. The locus identified modifies splicing of *BIRC6* in
36 stimulated monocytes, implicating regulation of apoptosis and autophagy in the pathogenesis of
37 sepsis in Kenyan children.

39 Introduction

40 Invasive bacterial diseases are a major cause of child morbidity and mortality in Africa (*Berkley*
41 *et al., 2005*). Although improved control measures, including the rollout of anti-bacterial conju-
42 gate vaccines (*Cowgill et al., 2006; Silaba et al., 2019*), have led to recent declines, the burden of
43 conditions such as pneumonia, meningitis and sepsis secondary to bacterial pathogens remains
44 significant (*Vos et al., 2020*). A better understanding of the biology of invasive bacterial infections
45 in African populations might help the development of novel interventions.

46 Susceptibility to invasive bacterial infections varies widely between individuals. In African chil-
47 dren, some of this variability is determined by acquired comorbidities such as HIV, malnutrition and
48 malaria (*Berkley et al., 2005; Church and Maitland, 2014; Scott et al., 2011*). However, the identi-
49 fication of common genetic variants as determinants of bacterial infection suggests that a signifi-
50 cant portion of this variability is heritable. Many of these genetic susceptibility loci have pathogen-
51 specific effects (*Davila et al., 2010; Gilchrist et al., 2018; Rautanen et al., 2016*), which is consistent
52 with our understanding of infection susceptibility derived from primary immunodeficiencies. Key
53 examples of pathogen-specificity among primary immunodeficiencies include Mendelian suscep-
54 tibility to mycobacterial disease and susceptibility to non-tuberculous mycobacteria and nonty-
55 phoidal *Salmonella* (*Bustamante et al., 2014*), terminal complement deficiencies and meningococ-
56 cal disease (*Figueroa et al., 1993*), and IRAK4 deficiency and pneumococcal disease (*Picard et al.,*
57 *2007*). A major exception to this is the rs334 A>T mutation in *HBB* (sickle haemoglobin), which is as-
58 sociated with raised and lowered risks of infection secondary to a broad range of pathogens among
59 homozygotes (*Williams et al., 2009*) and heterozygotes (*Scott et al., 2011*) respectively. However,
60 the effect sizes associated with sickle haemoglobin are extreme, being maintained in populations
61 by balancing selection, and larger sample sizes will probably be needed for the discovery of new
62 variants with multi-pathogen effects.

63 Because the clinical features of invasive bacterial infections and severe malaria are broadly sim-
64 ilar (*Bejon et al., 2007*), it can be difficult to distinguish between severe illness caused by extensive
65 sequestration of malaria parasites in the microvasculature ('true' severe malaria) and bacterial seps-
66 is in the presence of incidental parasitaemia on the basis of clinical features alone. This is made
67 harder still by the fact that antibiotic pre-treatment and inadequate blood-culture volumes mean
68 that, even in settings with excellent diagnostic facilities, true invasive bacterial infections can often
69 not be confirmed (*Driscoll et al., 2017*). Recently, we illustrated this clinical complexity through a
70 study in which we used probabilistic models based on malaria-specific biomarkers to show that
71 approximately one third of children recruited to studies in Africa with a clinical diagnosis of severe
72 malaria were actually suffering from other conditions (*Watson et al., 2021a,b*).

73 In the current study, we extend this work to show that invasive bacterial infections are common
74 in children admitted to hospital with a clinical diagnosis of severe malaria, but in whom biomarkers
75 subsequently suggest that malaria was probably not the primary cause for their severe illness. We
76 then construct a dataset of genome-wide genotyped samples from 5,400 Kenyan children, compris-
77 ing critically unwell Kenyan children with bacteraemia (*Rautanen et al., 2016*) and severe malaria
78 (*Band et al., 2019*), and population controls. Using this dataset we perform a GWAS of invasive bac-
79 terial infection in Kenyan children, weighting cases according to the probability that their disease
80 was mediated by a bacterial pathogen. In doing so, we increase our study power and identify *BIRC6*
81 as a novel genetic determinant of invasive bacterial disease in Kenyan children.

82 Results

83 Severe malaria probability and risk of bacteraemia

84 Children admitted to the high dependency ward of Kilifi County Hospital with a clinical diagnosis
85 of severe malaria, defined as a severe febrile illness in the presence of *P. falciparum* parasitaemia
86 (n=2,200), between 11th June 1995 and 12th June 2008 were included in the study. While this
87 definition is sensitive it is not specific, meaning that our study will have included some children

Table 1. Demographics & clinical characteristics of Kenyan children with severe malaria.

| Model | Numbers | Sex (female) | Age (months) | Bacteraemia | Mortality |
|--------------------|--------------------------|---------------|--------------|-------------|-------------|
| <i>Pf</i> HRP2/Plt | Total (n=1,400) | 695 (49.6%) | 29 (17-44) | 51 (3.6%) | 155 (11.1%) |
| | P(SM Data)>0.5 (n=975) | 497 (51.0%) | 29 (18-45) | 23 (2.4%) | 94 (7.4%) |
| | P(SM Data)<0.5 (n=425) | 198 (46.6%) | 28 (16-43) | 28 (6.6%) | 61 (14.4%) |
| WBC/Plt | Total (n=2,220) | 1,074 (48.4%) | 28 (15-43) | 78 (3.5%) | 256 (11.6%) |
| | P(SM Data)>0.5 (n=1,279) | 623 (48.7%) | 29 (17-44) | 32 (2.5%) | 106 (8.4%) |
| | P(SM Data)<0.5 (n=941) | 451 (47.9%) | 25 (13-40) | 46 (4.9%) | 150 (15.9%) |

Mortality reflects in-patient deaths. Figures are absolute numbers with percentages or interquartile ranges in parentheses. P(SM|Data) reflects the probability of 'true' severe malaria estimated from each model (*Pf*HRP2/Platelet count, White blood cell count/Platelet count).

88 with sepsis accompanied by incidental parasitaemia (*Watson et al., 2021a*). We therefore used
 89 two probabilistic models, which included either platelet counts and plasma *Pf*HRP2 concentrations
 90 (Model 1, n=1,400) or white blood cell and platelet counts (Model 2, n=2,200), to determine the
 91 likelihood of 'true' severe malaria among these children. The estimated probabilities of 'true' severe
 92 malaria using each model were well-correlated ($r = 0.64$). Of 1,400 children with a clinical diagnosis
 93 of severe malaria with measured plasma *Pf*HRP2 concentrations, 425 (30.4%, Figure 1A and 1B)
 94 had a low probability (P(SM|Data)<0.5) of having 'true' severe malaria (941 of 2,220 children using
 95 WBC and platelet count data, Figure 1-figure supplement 1A and 1B). That is, while they presented
 96 with febrile illness and concomitant malaria parasitaemia, it is unlikely that their illnesses were
 97 directly attributable to malaria.

98 In keeping with the hypothesis that a significant proportion of these critically unwell children
 99 represented culture-negative invasive bacterial disease (Figure 1), in-patient mortality was higher
 100 among children with a low than a high probability of 'true' severe malaria (Table 1; $OR_{model1} = 1.57$,
 101 95% CI 1.11 – 2.21, $p = 0.01$; $OR_{model2} = 2.09$, 95% CI 1.60 – 2.72, $p = 4.91 \times 10^{-8}$). This was also
 102 reflected in the rates of concurrent bacteraemia (Table 1; $OR_{model1} = 2.92$, 95% CI 1.66 – 5.13, $p =$
 103 1.07×10^{-4} ; $OR_{model2} = 2.00$, 95% CI 1.27 – 3.17, $p = 0.003$). Similarly, the constituents of model 1
 104 were each associated with blood culture positivity, both higher platelet counts (OR=2.36, 95% CI
 105 1.19-4.70, $p = 0.014$) and lower *Pf*HRP2 levels (OR=0.52, 95% CI 0.39-0.70, $p = 9.62 \times 10^{-6}$) both
 106 being associated with the risk of coincident bacteraemia (Figure 1C and 1D). Conversely, white
 107 blood counts in isolation were not associated with risk of concurrent bacteraemia (Figure 1-figure
 108 supplement 1). Plasma *Pf*HRP2 is the single best biomarker for severe malaria (*Hendriksen et al.,*
 109 **2012**). In light of this, and given the greater enrichment for concurrent bacteraemia among children
 110 with a low probability of 'true' severe malaria as calculated by Model 1 than Model 2, we used Model
 111 1 probabilities in downstream analyses where available (n=1,400) and used Model 2 probabilities
 112 for all other cases (n=800).

113 **GWAS of invasive bacterial disease in Kenyan children**

114 Children with a clinical diagnosis of severe malaria but a low probability of having 'true' severe
 115 malaria, are thus enriched for invasive bacterial disease. Motivated by this observation we per-
 116 formed a genome-wide association study of invasive bacterial infection in Kenyan children in which
 117 we included both children with culture-confirmed bacteraemia and children with a clinical diagno-
 118 sis of severe malaria. Children admitted to Kilifi County Hospital between 1st August 1998 and
 119 30th October 2010 with community-acquired bacteraemia were recruited to the study as well as
 120 children from the severe malaria study described above. Control children were recruited from
 121 the same population between 1st August 2006 and 30th December 2010 as described in detail
 122 previously (*Scott et al., 2011*).

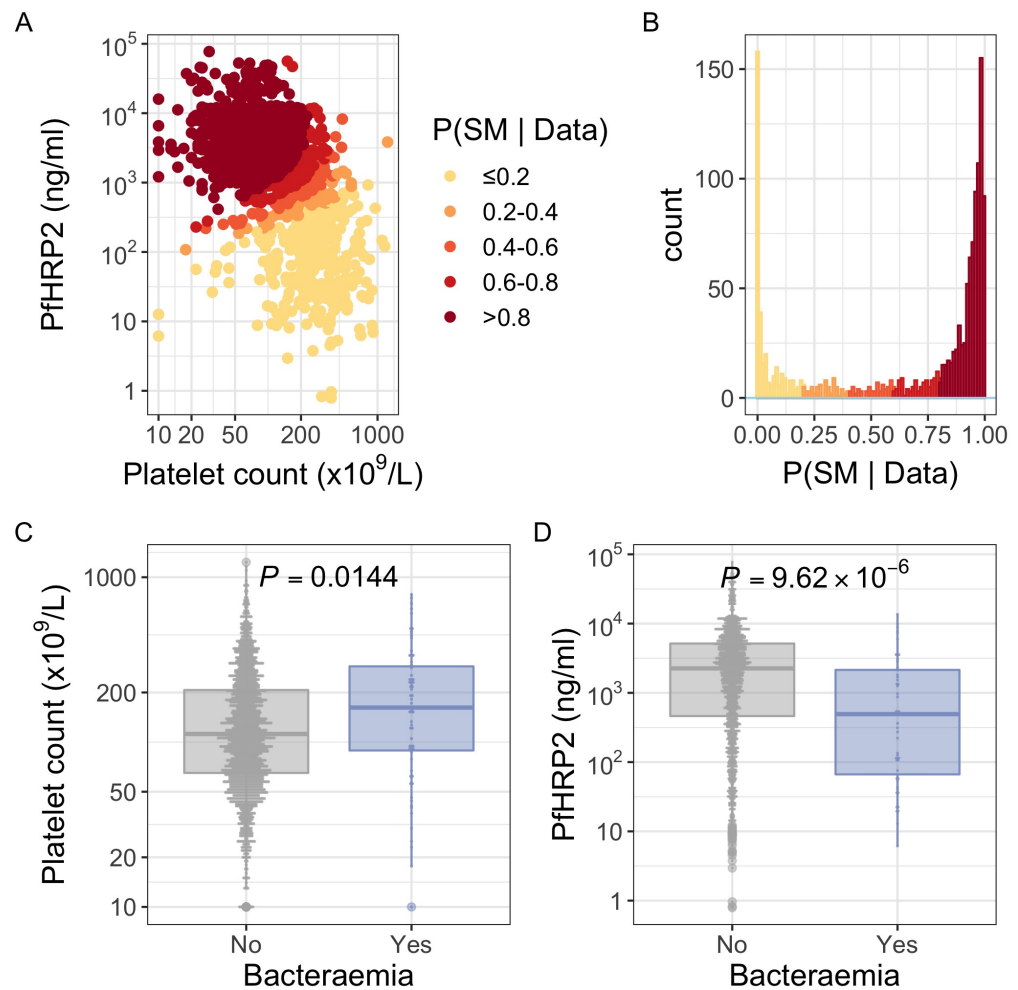


Figure 1. *PfHRP2* and platelet count as predictors of severe malaria. (A) Distribution of *PfHRP2* concentrations and platelet count among Kenyan children ($n=1,400$) with a clinical diagnosis of severe malaria. Points are coloured according to the probability of 'true' severe malaria given the data. (B) Distribution of 'true' severe malaria probabilities estimated from platelet count and plasma *PfHRP2* concentrations. (C) Platelets counts in children with a clinical diagnosis of severe malaria with and without concomitant bacteraemia. (D) *PfHRP2* concentrations in children with a clinical diagnosis of severe malaria with and without concomitant bacteraemia.

Figure 1-Figure supplement 1. White blood cell and platelet count as predictors of severe malaria. (A) Distribution of white blood cell and platelet count among Kenyan children ($n=2,200$) with a clinical diagnosis of severe malaria. Points are coloured according to the probability of 'true' severe malaria given the data. (B) Distribution of 'true' severe malaria probabilities estimated from platelet count and white blood cell count. (C) Platelets counts in children with a clinical diagnosis of severe malaria with and without concomitant bacteraemia. (D) White blood cell counts in children with a clinical diagnosis of severe malaria with and without concomitant bacteraemia.

Table 2. Demographics & clinical characteristics of GWAS study samples.

| | | Numbers | Sex (female) | Age (months) | Genotyping platform |
|----------------|-----------------------------------|-------------|--------------|----------------|-------------------------------------|
| Bacteraemia | Overall | 1,445 | 614 (42.5%) | 14 (5-34) | Affy SNP 6.0 |
| | <i>Acinetobacter</i> | 118 | 45 (38.1%) | 13 (3-28) | |
| | β -haemolytic <i>Strep.</i> | 130 | 60 (46.2%) | 5 (1-20) | |
| | <i>E. coli</i> | 141 | 58 (41.1%) | 11 (6-25) | |
| | Hib | 113 | 53 (46.9%) | 12 (5-25) | |
| | NTS | 159 | 75 (47.2%) | 15 (9-26) | |
| | <i>S. pneumoniae</i> | 390 | 151 (38.7%) | 23 (9-61) | |
| | <i>S. aureus</i> | 152 | 64 (42.1%) | 26 (9-88) | |
| Other | 242 | 110 (45.5%) | 10 (1-28) | | |
| Severe Malaria | Overall | 1,143 | 559 (48.9%) | 27 (16-41) | Omni 2.5M |
| | P(SM Data)<0.5 | 375 | 176 (46.9%) | 28 (17-42) | |
| | P(SM Data)>0.5 | 768 | 383 (49.9%) | 26 (15-40) | |
| Controls | | 2,812 | 1,406 (50%) | * 917 (33%) | 1,895 Affy SNP 6.0 917 Omni 2.5M |

P(SM | Data) reflects the probability of 'true' severe malaria estimated from *Pf*HRP2 concentration and platelet count or white blood cell count and platelet count.

*Control children were recruited between 3 and 12 months of age and have been subject to longitudinal follow-up.

123 Following quality control measures (see Materials and Methods), we included 1,445 cases of
 124 culture-confirmed bacteraemia, 1,143 cases of severe malaria and 2,812 control children in our cur-
 125 rent analysis (Table 2). To account for the varying proportion of invasive bacterial disease among
 126 severe malaria cases, we applied weights to our regression analysis to reflect the greater likelihood
 127 of invasive bacterial disease among children with a low probability of 'true' severe malaria (sam-
 128 ple weight, $w = 1 - P(SM | Data)$). Where *Pf*HRP2 concentrations were available (n=909) we used
 129 *Pf*HRP2 and platelet count to determine $P(SM | Data)$ while we used white cell and platelet counts
 130 (n=234) in cases where they were not available. Cases with culture-proven bacteraemia and control
 131 samples were assigned a sample weight of $w = 1$. Inclusion of the 6 major principal components
 132 of genotyping data and genotyping platform as covariates in the model adequately controlled for
 133 confounding variation ($\lambda = 1.0208$, Figure 2-figure supplement 1). In that analysis we found evi-
 134 dence supporting an association between risk of invasive bacterial disease in Kenyan children and
 135 7 SNPs at a single locus on chromosome 2 (peak SNP: rs183868412:T, OR=2.13, 95% CI 1.65-2.74,
 136 $p = 4.64 \times 10^{-9}$) (Figure 2, Table 3). Fine-mapping of this association identified a credible set of 7
 137 SNPs with a 95% probability of containing the causal variant (Table 3), spanning a 212kb region:
 138 chr2:32,402,640-32,614,746.

139 We sought to replicate evidence of association in our discovery analysis through use of an inde-
 140 pendent case-control collection of Kenyan children with bacteraemia (n=434) and healthy controls
 141 (n=1,258) conducted in the same population. The peak trait-associated variants in the discovery
 142 analysis were well-imputed in the replication data (rs183868412 imputation info score = 0.84). In
 143 that analysis, we found evidence supporting the association at chromosome 2 with invasive bacte-
 144 rial disease (Figure 3, Table 4: rs183868412:T, OR=2.77, 95% CI 1.49-5.12, $p = 1.29 \times 10^{-3}$). In a fixed
 145 effects meta-analysis, rs183868412:T was strongly associated with risk of invasive bacterial disease
 146 in Kenyan children: OR=2.21, 95% CI 1.75-2.79, $p = 2.42 \times 10^{-11}$. That association was driven by chil-
 147 dren with culture-confirmed bacteraemia and critically unwell children with malaria parasites, but
 148 a low probability of 'true' severe malaria. In a stratified analysis (Figure 3, Table 4), rs183868412

Table 3. 95% credible SNP set of invasive bacterial disease association.

| SNP | Effect allele | Chr | BP | MAF | Info score | OR (95% CI) | p-value |
|-------------|---------------|-----|------------|-------|------------|------------------|-----------------------|
| rs183868412 | T | 2 | 32,478,169 | 0.021 | 0.956 | 2.13 (1.65-2.74) | 4.64×10^{-9} |
| rs139827594 | G | 2 | 32,402,640 | 0.020 | 0.966 | 2.12 (1.65-2.73) | 4.96×10^{-9} |
| rs144257579 | G | 2 | 32,507,619 | 0.021 | 0.954 | 2.11 (1.64-2.72) | 6.82×10^{-9} |
| rs145056232 | C | 2 | 32,503,024 | 0.021 | 0.955 | 2.11 (1.64-2.72) | 6.86×10^{-9} |
| rs145315025 | G | 2 | 32,502,654 | 0.021 | 0.955 | 2.11 (1.64-2.72) | 6.87×10^{-9} |
| rs143909151 | T | 2 | 32,531,452 | 0.021 | 0.962 | 2.11 (1.64-2.71) | 8.01×10^{-9} |
| rs150430979 | T | 2 | 32,614,746 | 0.021 | 0.955 | 2.11 (1.64-2.72) | 8.18×10^{-9} |

MAF, minor allele frequency. CI, confidence interval. Genomic coordinates are GRCh38.

Table 4. Effect of rs183868412 genotype on risk of invasive bacterial disease in Kenyan children.

| | | Numbers | Genotypes | MAF | OR (95% CI) | p-value |
|---------------|----------------------|---------|-------------|-------|------------------|----------------------------|
| Discovery | Overall | 2,588 | 3/164/2,421 | 0.033 | 2.13 (1.65-2.74) | $p = 4.64 \times 10^{-9}$ |
| | Bacteraemia* | 1,445 | 3/125/1,317 | 0.045 | 2.12 (1.60-2.82) | $p = 1.94 \times 10^{-7}$ |
| | SM - P(SM Data)<0.5* | 375 | 0/20/355 | 0.027 | 2.37 (1.27-4.43) | $p = 6.82 \times 10^{-3}$ |
| | SM - P(SM Data)>0.5* | 768 | 0/19/749 | 0.012 | 1.07 (0.57-2.01) | $p = 0.823$ |
| | Controls | 2,812 | 0/111/2,701 | 0.020 | | |
| Replication | Cases | 434 | 0/24/410 | 0.028 | 2.77 (1.49-5.12) | $p = 1.29 \times 10^{-3}$ |
| | Controls | 1,258 | 0/28/1,230 | 0.011 | | |
| Meta-analysis | Cases | 3,022 | 3/188/2,831 | 0.032 | 2.21 (1.75-2.79) | $p = 2.42 \times 10^{-11}$ |
| | Controls | 4,070 | 0/139/3,931 | 0.017 | | |

*estimates derived from multinomial logistic regression model. P(SM|Data) represent the probability of 'true' severe malaria estimated from plasma *Pf*HRP2 concentration and platelet count (n=909) or white blood cell count and platelet count (n=234). SM, severe malaria. MAF, minor allele frequency. CI, confidence interval.

149 was associated with culture-confirmed bacteraemia (OR=2.12, 95% CI 1.60-2.82, $p = 1.94 \times 10^{-7}$) and
 150 critical illness with parasitaemia and with a low probability of 'true' severe malaria (P(SM|Data)<0.5:
 151 OR=2.37, 95% CI 1.27-4.43, $p = 6.82 \times 10^{-3}$), but was not associated with risk of critical illness with a
 152 high probability of 'true' severe malaria (P(SM|Data)>0.5: $p = 0.823$).

153 The genetic variants associated with invasive bacterial disease in Kenyan children are monomor-
 154 phic in non-African populations (<https://gnomad.broadinstitute.org>). Within Africa, rs183868412:T is
 155 present in all 9 African populations included in the MalariaGEN consortium project (*Band et al.,*
 156 **2019**) (Table 5), minor allele frequencies ranging from 0.011 in The Gambia to 0.034 in Malawi.
 157 There is no evidence for within-Africa differentiation at rs183868412 ($p = 0.601$).

158 **rs183868412 is associated with risk of invasive bacterial disease secondary to di-**
 159 **verse pathogens and is independent of malaria.**

160 Previous data describing the genetic risk of invasive bacterial disease in this population have iden-
 161 tified pathogen-specific effects. To better-understand the range of pathogens to which genetic
 162 variation at *BIRC6* modifies risk we estimated the effect of rs183868412 on the risk of bacteraemia
 163 caused by the seven most common causative pathogens within this population (Figure 4A). In that
 164 analysis, the data best-supported a model in which genotype increases risk of bacteraemia caused
 165 by a broad range of pathogens, including bacteraemia secondary to pneumococcus, nontyphoidal
 166 *Salmonellae*, *E. coli*, β -haemolytic *Streptococci*, *S. aureus* and other less common pathogens grouped
 167 as a single stratum (log10 Bayes factor= 4.72). Genotype at rs183868412 similarly modified risk of

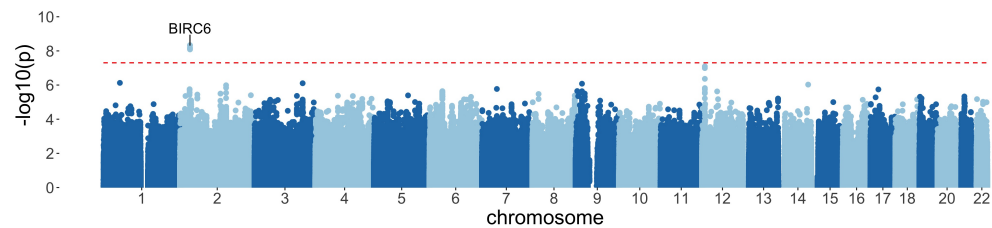


Figure 2. Manhattan plot of invasive bacterial infection in Kenyan children. Evidence for association with invasive bacterial disease at genotyped and imputed autosomal SNPs and indels ($n=14,010,600$) in Kenyan children (bacteraemia cases = 1,445, severe malaria cases = 1,143, controls = 2,812). Association statistics represent additive association. The red, dashed line denotes $p = 5 \times 10^{-8}$.

Figure 2-Figure supplement 1. Genotyping concordance between Illumina and Affymetrix platforms. Pairwise genotyping concordance between samples genotyped on both Affymetrix SNP 6.0 and Illumina Omni 2.5M platforms.

Figure 2-Figure supplement 2. Principal components of genome-wide genotyping data in discovery samples. Individuals are color-coded according to genotyping platform; Affymetrix SNP 6.0 in purple, Illumina Omni 2.5M in orange.

Figure 2-Figure supplement 3. Principal components of genome-wide genotyping data in discovery samples. Individuals are color-coded according to self-reported ethnicity; Chonyi in red, Giriama in blue, Kauma in green and other in grey.

Figure 2-Figure supplement 4. Quantile-quantile plot of invasive bacterial infection in Kenyan children. QQ plot of weighted logistic regression GWAS of invasive bacterial disease in Kenyan children (2,588 cases, 2,812 controls).

168 bacteraemia in the neonatal period and in older children (log₁₀ Bayes factor= 2.70, Figure 4B).

169 Malaria infection results in increased risk of invasive bacterial disease secondary to a broad
 170 range of pathogens (*Scott et al., 2011*), and genetic determinants of malaria risk (e.g. sickle cell
 171 trait) modify risk of bacterial infection in malaria-endemic settings (*Scott et al., 2011*). The ob-
 172 servation that, among children with a clinical diagnosis of severe malaria, risk of disease is only
 173 modified by rs183868412 in children with a low probability that their disease represents ‘true’ se-
 174 vere malaria (Figure 3) suggests that the effect of genetic variation at *BIRC6* on invasive bacterial
 175 disease risk operates independently of malaria. In keeping with this, the data best-supports an ef-
 176 fect of rs183868412 genotype on bacteraemia risk in children both with and without concomitant
 177 parasitaemia (log₁₀ Bayes factor= 2.73, Figure 4C). In addition, unlike sickle cell trait (*Scott et al.,*
 178 *2011*), the increased risk of invasive bacterial infection conferred by rs183868412:T carriage in the

Table 5. rs183868412 frequencies in Africa.

| Population | Number | MAF |
|--------------|--------|-------|
| Gambia | 2,605 | 0.011 |
| Mali | 183 | 0.021 |
| Burkina Faso | 596 | 0.009 |
| Ghana | 320 | 0.014 |
| Nigeria | 22 | 0.024 |
| Cameroon | 685 | 0.031 |
| Malawi | 1,317 | 0.034 |
| Tanzania | 402 | 0.028 |
| Kenya | 1,681 | 0.017 |

Numbers reflect healthy control samples. MAF, minor allele frequency.

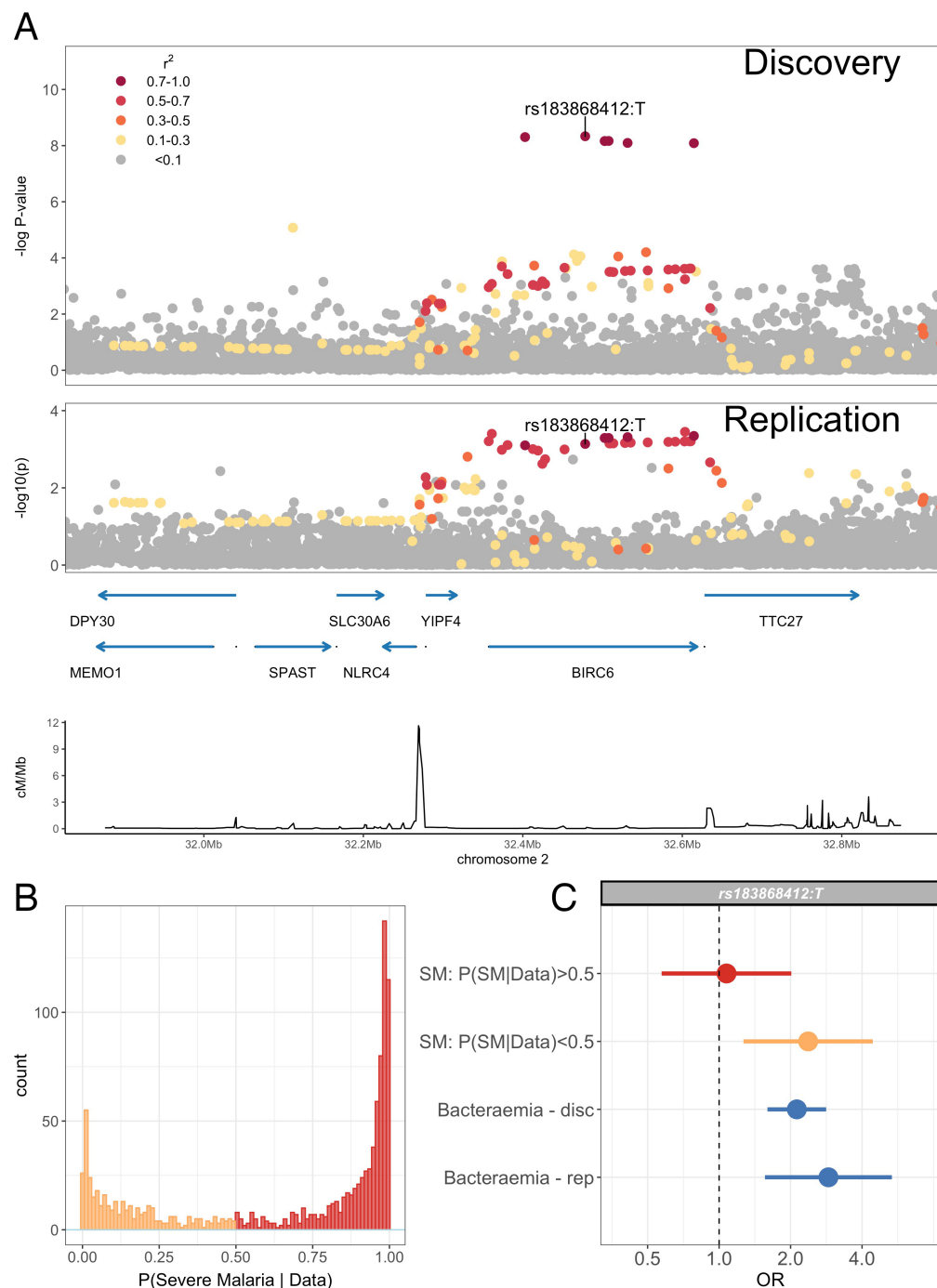


Figure 3. Association with invasive bacterial disease at the *BIRC6* locus. (A) Regional association plot of invasive bacterial disease association at the *BIRC6* locus in the discovery and replication analyses. SNPs are coloured according to linkage disequilibrium to rs183868412. Genomic coordinates are GRCh38. (B) Distribution of 'true' severe malaria probabilities among malaria cases estimated from plasma *Pf*HRP2 concentration and platelet count (n=909) and white blood cell count and platelet count (n=234). (C) Odds ratios and 95% confidence intervals of rs183868412 association with disease stratified by malaria cases with high (P>0.5, red) and low (P<0.5, orange) probabilities of 'true' severe malaria and culture-proven invasive bacterial disease (blue). P(SM | Data) represents the probability of 'true' severe malaria estimated from plasma *Pf*HRP2 concentration and platelet count (n=909) or white blood cell count and platelet count (n=234).

Figure 3-Figure supplement 1. Principal components of genome-wide genotyping data in replication samples. Individuals are color-coded according to self-reported ethnicity; Chonyi in red, Giriama in blue, Kauma in green and other in grey.

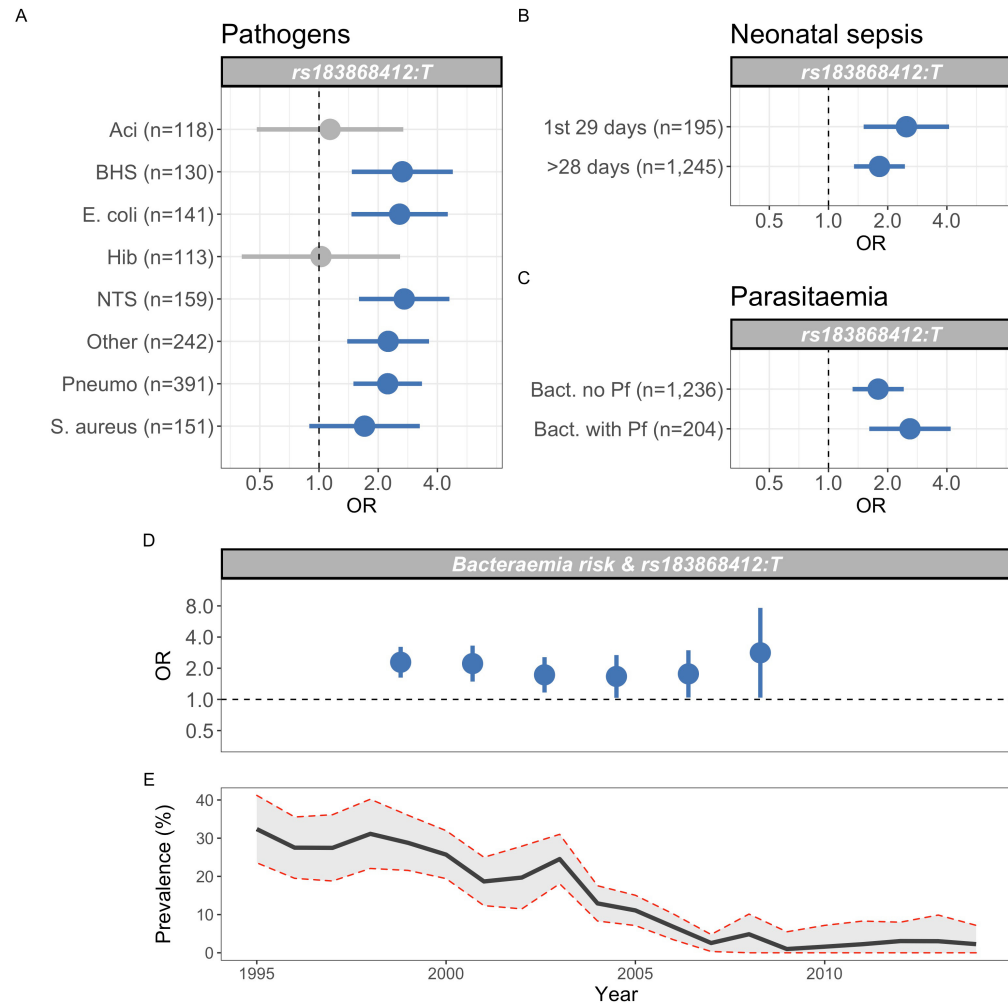


Figure 4. Genetic variation at *BIRC6* confers broad susceptibility to invasive bacterial disease. Odds ratios and 95% confidence intervals of rs183868412 association with invasive bacterial disease stratified by pathogen (A), neonatal and non-neonatal sepsis (B) and bacteraemia with and without malaria parasitaemia (C). Odds ratios and 95% confidence intervals of rs183868412 association with invasive bacterial disease stratified by year (D), compared to age-standardized, annual malaria parasite prevalence in Kilifi, Kenya, as estimated from parasite prevalence among trauma admissions (E). We compared models of association across strata using a Bayesian approach (see Methods). Strata associated with rs183868412 genotype in the most likely model in each analysis are highlighted in blue.

179 study setting is stable across a period of declining malaria prevalence (Bayes factor= 8.7, Figure
180 4D).

181 **rs183868412 is associated with alternative splicing of *BIRC6* in stimulated mono-** 182 **cytes.**

183 Trait associated genetic variation identified by GWAS is highly enriched for regulatory variation. The
184 African specificity of the trait-associated variation identified here makes annotation with publicly-
185 available regulatory mapping data challenging. To investigate the regulatory function of rs183868412
186 in immune cells in African populations we used eQTL mapping data from 200 (100 European and
187 100 African ancestry) individuals in primary monocytes with and without innate stimulation (*Quach*
188 *et al.*, 2016); influenza A virus, LPS, Pam3CSK4 (synthetic lipoprotein and TLR1/2 agonist) and R848
189 (a TLR7/8 agonist). In this dataset, we found no evidence for a regulatory effect of rs183868412
190 at the gene level in monocytes regardless of stimulation. We did, however, observe an effect of
191 rs183868412 genotype on expression of a 12bp *BIRC6* exonic sequence (chr2:32,453,943-32,453,954,
192 $p = 4.40 \times 10^{-5}$), with evidence for co-localisation of this eQTL with our GWAS signal (posterior
193 probability of colocalisation, PP4 = 0.937, Figure 5). This effect was only observed following stimu-
194 lation with Pam3CSK4 (Figure 5), with the bacteraemia risk allele, rs183868412:T, being associ-
195 ated with reduced expression of this sequence. That 12bp sequence is associated with an alter-
196 native splicing event that results in extension of a *BIRC6* exon. The 23rd exon (ENSE00001189810,
197 chr2:32,453,808-32,453,942) of the canonical *BIRC6* transcript, ENST00000421745.6, is 135bp long
198 and terminates immediately before the 12bp sequence associated with rs183868412:T genotype.
199 The 22nd exon (ENSE00003835010, chr2:32,453,808-32,453,942) of an alternative *BIRC6* transcript,
200 ENST00000648282.1, is 147bp long, having the same start site but including the 12bp sequence
201 at its 3' end. Thus, increased risk of invasive bacterial disease may be associated with decreased
202 expression of an alternative *BIRC6* transcript in TLR1/2 stimulated monocytes.

203 **Discussion**

204 In this study, we have leveraged the close relationship between *P. falciparum* infection and bacter-
205 aemia in African children (*Scott et al.*, 2011) to perform a GWAS of invasive bacterial infection in
206 5,400 Kenyan children. We approached this by defining the probability with which each critically
207 unwell child with a clinical diagnosis of severe malaria has a disease process directly mediated by
208 malaria, that is 'true' severe malaria. We hypothesised that critically unwell children, with a low
209 probability of having 'true' severe malaria, are enriched for invasive bacterial infections. We ex-
210 plored the validity of this approach, demonstrating that children with a low probability of 'true'
211 severe malaria were indeed enriched for culture-proven bacteraemia and were at a higher risk of
212 death than children with a higher probability. We therefore performed a GWAS weighting cases
213 according to their likelihood of invasive bacterial disease. In doing so, we have identified and vali-
214 dated *BIRC6* as a novel genetic susceptibility locus for all-cause invasive bacterial disease in Kenyan
215 children.

216 The disease-associated locus modifies risk of invasive bacterial disease caused by a broad range
217 pathogens, including β -haemolytic *Streptococci*, *E. coli*, nontyphoidal *Salmonella*, *S. pneumoniae* and
218 *S. aureus*. Moreover it modifies risk of invasive infection in both the neonatal period and in older
219 children. Furthermore, in contrast to the rs334 *HBB* A>T mutation (*Scott et al.*, 2011), rs183868412
220 modifies risk of invasive bacterial disease in a manner independent of malaria, with rs183868412:T
221 carriage increasing risk of disease across a period of falling malaria transmission and in children
222 with and without concurrent parasitaemia.

223 We further demonstrate that rs183868412 mediates risk of invasive bacterial disease through
224 the modification of *BIRC6* splicing in Pam3CSK4-stimulated monocytes. *BIRC6* (Baculovirus inhibitor
225 of apoptosis protein repeat containing 6), also known as *BRUCE* (BIR repeat containing ubiquitin-
226 conjugating enzyme), encodes a large member of the inhibitor of apoptosis protein (IAP) family

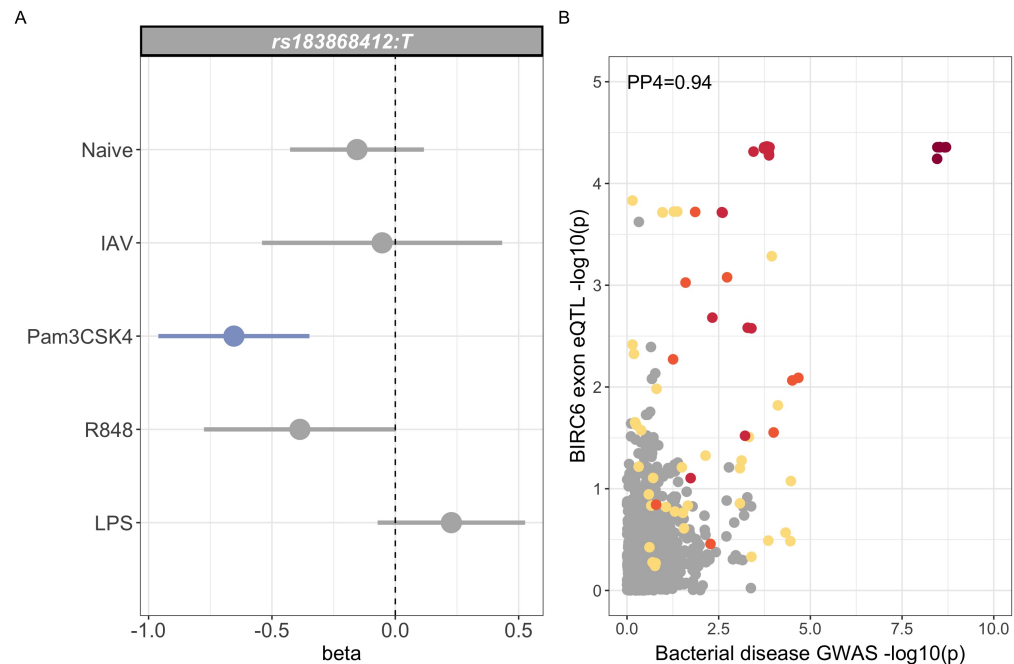


Figure 5. Regulatory function of rs183868412 in monocytes. (A) Betas and 95% confidence intervals of rs183868412 association with expression of a 12bp *BIRC6* exon (chr2:32,453,943-32,453,954) in monocytes. Monocytes are naive or stimulated with; LPS (lipopolysaccharide), IAV (influenza A virus), Pam3CSK4 and R848. (B) Colocalisation of the *BIRC6* exon eQTL in Pam3CSK4-stimulated monocytes colocalizes with the risk locus for invasive bacterial disease ($PP4 = 0.937$). SNPs are coloured according to linkage disequilibrium to rs183868412.

227 (*Hauser et al., 1998*). Members of the IAP family bind to cognate caspases, inhibiting their activity,
228 and thereby cell death, through occlusion of their active site (*Verhagen et al., 2001*). A proportion
229 of IAPs also contain an E3 ubiquitin ligase allowing both direct inhibition of caspases and targeting
230 of caspases for proteasomal degradation (*Verhagen et al., 2001*). *BIRC6* contains both inhibitor of
231 apoptosis domains and an E2/E3 ubiquitin ligase, which function to inhibit apoptosis in response
232 to a variety of stimuli, both by interaction with and degradation of caspase-9, but also through the
233 ubiquitination and degradation of SMAC, an IAP antagonist (*Hao et al., 2004; Bartke et al., 2004*).
234 *BIRC6* also regulates autophagosome-lysosome fusion (*Ebner et al., 2018*), and ubiquitinates (and
235 targets for degradation) LC3, a key effector of autophagosome formation. Thus, *BIRC6* also acts as
236 a negative regulator of autophagy (*Jia and Bonifacino, 2019*).

237 It is highly plausible that *BIRC6* could determine susceptibility to invasive infection through ei-
238 ther its regulation of apoptosis or autophagy (or both). Sepsis induces marked changes in apopto-
239 sis across a range of immune cells (*Hotchkiss and Nicholson, 2006*). There is markedly enhanced
240 apoptosis in both dendritic cells (*Hotchkiss et al., 2002*) and in lymphocytes. Enhanced lymphocyte
241 apoptosis is most striking in B cells and CD4⁺ T cells (*Hotchkiss et al., 2001*) which, at least in part,
242 is mediated by caspase-9. The consequent lymphopenia is correlated with both severity of sepsis
243 and outcome (*Le Tulzo et al., 2002*). In addition to the direct effects of immune cell loss on the
244 innate and adaptive immune responses to invasive infection, sepsis-induced apoptosis induces im-
245 mune cell dysfunction, phagocytosis of apoptotic cells resulting in reduction in pro-inflammatory
246 cytokine production and cross-presentation of antigen from apoptotic cells to adaptive immune
247 cells (*Albert, 2004*). In keeping with a role for regulators of apoptosis in the pathogenesis of sepsis,
248 members of the IAP family, including *NAIP/BIRC1* and *BIRC3*, are downregulated in immune cells
249 in patients with sepsis, as is the *BIRC6* ubiquitination target *SMAC* (*Hoogerwerf et al., 2010*). Au-
250 topagy contributes to the direct removal of intracellular pathogens and, through the degradation

251 of invading organisms in autophagosomes, directs antigen presentation and pro-inflammatory cy-
252 tokine secretion (*Deretic et al., 2013*). As above, *BIRC6* regulates autophagy through its interaction
253 with LC3, and overexpression of *LC3B* limits inflammation and tissue injury in a mouse model of
254 sepsis (*Lo et al., 2013*).

255 In keeping with a role for *BIRC6* in autophagy and apoptosis in sepsis, our data identify a role
256 for genetic variation at *BIRC6* in determining risk of invasive infection secondary to a broad range
257 of bacteria. This is in contrast to previously-published data describing susceptibility to invasive
258 bacterial infection, which has highlighted a prominent role for genetic risk factors that are spe-
259 cific to single pathogens (*Davila et al., 2010; Gilchrist et al., 2018; Rautanen et al., 2016*). In this
260 study, the derived allele (T) at rs183868412 was associated with increased risk of bacteraemia sec-
261 ondary to gram positive (β -haemolytic *Streptococci*, *S. pneumoniae* and *S. aureus*) and gram nega-
262 tive (*E. coli*, nontyphoidal *Salmonella*) pathogens, including intracellular and extracellular bacteria,
263 and enteric and respiratory pathogens. Moreover, rs183868412 modified risk of bacteraemia in
264 both the neonatal period, when infection is likely to be maternally derived, and in older children,
265 when sources of community acquired infection will be more diverse. This modulation of invasive
266 bacterial disease risk, despite diverse sources and routes of infection and diverse mechanisms of
267 invasion, suggests a mechanism in which genetic variation at *BIRC6* modifies risk of invasive infec-
268 tion downstream of initial mechanisms of infection and invasion. The African-specific nature of the
269 trait-associated variation identified here limits our ability to comprehensively interrogate the effect
270 of that variation in immune cells. The eQTL mapping data that we utilise here (*Quach et al., 2016*) is
271 limited in that it allows us only to consider a single immune cell type. A more complete understand-
272 ing of the role played by genetic variation at *BIRC6* plays in the pathogenesis of sepsis in African
273 children will require more detailed expression and functional studies in African populations.

274 Taken together, our data identify a role for *BIRC6* in the pathogenesis of invasive bacterial in-
275 fections in Kenyan children. By maximising our available sample size to include children with a
276 high likelihood of invasive bacterial infection, but without culture-confirmed infection, we facilitate
277 novel variant discovery and reveal a common genetic architecture of invasive bacterial disease
278 secondary to diverse pathogens. In doing so we expand our understanding of the biology of inva-
279 sive infection in African children. In particular, these data inform our understanding of the biology
280 shared by diverse bacterial infections causing a common clinical syndrome: sepsis.

281 **Materials and Methods**

282 **Study samples**

283 Recruitment of the severe malaria cases, bacteraemia cases and healthy controls have been de-
284 scribed in detail elsewhere (*Ndila et al., 2018; Rautanen et al., 2016*). In brief, children under 14
285 years admitted to the high dependency ward of Kilifi County Hospital with a clinical diagnosis of
286 severe malaria, defined as *P. falciparum* parasites on blood film and at least one of; reduced Blan-
287 tyre Coma Score, severe anaemia (Hb<50g/L), evidence of respiratory distress, hypoglycaemia or
288 hyperparasitaemia were eligible for recruitment as cases of severe malaria. During the study pe-
289 riod, all children admitted to hospital, with the exception of elective surgical admissions and minor
290 trauma, had a blood sample taken for bacterial culture (BACTEC 9050 instrument, Becton Dickin-
291 son, USA). Children under 14 years, in whom a pathogenic organism was identified in blood were
292 eligible for study inclusion (*Bacillus* species, coryneform bacteria, coagulase-negative *Staphylococci*,
293 *Staphylococcus saprophyticus* and Viridans group *Streptococci* were considered contaminants). Con-
294 trol children were recruited between 3 and 12 months of age from consecutive live births from the
295 population which Kilifi County Hospital serves. Control children have been subject to longitudinal
296 follow-up.

297 **Models to define the probability of 'true' severe malaria.**

298 Among cases of severe malaria recruited to the study, we used probabilistic models to assign a
299 probability of that child's clinical presentation being mediated by parasite sequestration, that is
300 'true' severe malaria, as described previously (*Watson et al., 2021a,b*). Where available (n=1,400),
301 we used platelet counts and PfHRP2 concentrations to derive the probabilistic model. In cases
302 where PfHRP2 concentration was not measured (n=800), we used white blood cell counts and
303 platelet counts as input data to the model.

304 For both models (Model 1: PfHRP2/platelet counts; Model 2: platelet counts/white blood cell
305 counts), the probabilities of 'true' severe malaria were derived by fitting parametric latent class
306 models. These assumed that each patient had a binary latent state (true severe malaria versus not
307 severe malaria). For the Model 1, we assumed that in each latent state the data were distributed as
308 a single bivariate normal distribution. For the model 2, the data did not fit well to a two-component
309 bivariate normal (white blood cell counts have much weaker diagnostic value) so we assumed that
310 the data had bivariate student-t distribution for the severe malaria state, and a flexible mixture of
311 bivariate normals for the not severe malaria state.

312 **Genotyping & imputation**

313 For the discovery analysis, we utilised genotypes generated as part of genome-wide association
314 studies of severe malaria (*Band et al., 2019*) and bacteraemia (*Rautanen et al., 2016*) previously
315 reported in this population. Bacteraemia cases and controls were genotyped using the Affymetrix
316 SNP 6.0 array and the severe malaria samples using the Illumina Omni 2.5 M platform. SNP and
317 sample quality control for both datasets are highly analogous, and have been described previously
318 (*Band et al., 2019; Rautanen et al., 2016*). In brief, MalariaGEN SNP QC excluded poorly geno-
319 typed SNPs using the following metrics; SNP missingness >2.5%, minor allele frequency (MAF) <1%,
320 Hardy-Weinberg equilibrium (HWE) $p < 1 \times 10^{-20}$, plate effect $p < 1 \times 10^{-3}$ and a recall test quantify-
321 ing changes in genotype following a re-clustering process $p < 1 \times 10^{-6}$. For Affymetrix-genotyped
322 samples, SNP QC excluded SNPs outside the following QC thresholds; SNP missingness >2%, MAF
323 <1%, genotype probability (info) >0.975, plate effect $p < 1 \times 10^{-6}$, and HWE $p < 1 \times 10^{-20}$. Sam-
324 ple QC on both platforms excluded sample outliers with respect to channel intensity, missingness,
325 heterozygosity, population outliers and duplicated samples (IBD>0.75). In addition, for Affymetrix-
326 genotyped samples, samples were excluded in cases of discordant sex as recorded in the clinical
327 record and imputed from mean intensities from X and Y chromosome markers.

328 To facilitate combining datasets we applied an additional set of cross-platform QC procedures.
329 We defined a shared subset of SNPs genotyped and passing SNP QC on both platforms (n=167,108),
330 observing high levels of genotype concordance (median concordance 0.993, Figure 2-figure sup-
331 plement 1) among the subset of samples genotyped on both platforms (n=1,365). We used this
332 shared SNP set to compute relatedness estimates and PCs in PLINK v1.90 (*Chang et al., 2015*). The
333 major six PCs of shared genotypes differentiate self-reported ethnicity (Figure 2-figure supplement
334 2) and are non-differential with respect to genotyping platform (Figure 2-figure supplement 3). To
335 harmonise QC across both platforms we excluded MalariaGEN samples with discordant clinical
336 and genetic sex (n=136). We further excluded one of duplicate or related sample pairs (IBD>0.2)
337 across platforms, retaining case samples where possible and excluding equal numbers of con-
338 trol samples genotyped on each platform (n=1,973). Following QC, genotypes were phased using
339 SHAPEIT2 (*Delaneau et al., 2012*), and untyped genotypes imputed genome-wide using IMPUTE2
340 (v2.3.2) (*Howie et al., 2011, 2009*) with 1000 Genomes Phase III as a reference panel. Following
341 imputation, we excluded SNPs with imputation info scores <0.5, MAF <1% and HWE $p < 1 \times 10^{-5}$,
342 applying each threshold for each platform and overall. Following SNP and sample QC, 14,010,600
343 autosomal SNPs and indels from 5,400 samples (1,445 bacteraemia cases, 1,143 severe malaria
344 cases and 2,812 control samples: 917 Illumina genotyped and 1,895 Affymetrix genotyped) were
345 taken forward as a combined discovery dataset for association analysis.

346 **Association analysis & fine mapping**

347 In the discovery analysis, we tested for association between genotype at each variant passing QC
348 and invasive bacterial disease by logistic regression in an additive linear model. We used weighted
349 logistic regression to reflect the probability of each case sample being a 'true' case of invasive bac-
350 terial infection. Cases of culture-confirmed bacteraemia we assigned a weight of 1, whereas cases
351 of severe malaria were assigned weights $1 - P(\text{SM} | \text{Data})$, re-weighting the contribution of a case to
352 the log-likelihood according to its probability of representing invasive bacterial infection. Control
353 samples were assigned a weight of 1. Our regression thus assumes that the lower the probability
354 of 'true' severe malaria, the greater the probability that a case represents culture-negative invasive
355 bacterial disease. To control for confounding variation, we included the 6 major PCs of genotyping
356 data and genotyping platform as covariates in the model. Weighted logistic regression was imple-
357 mented using the *glm* function in R. As described previously (*Watson et al., 2021a*), standard errors
358 were transformed to reflect the reduced effective sample size resulting from inclusion of sample
359 weights in the model. We considered $p < 5 \times 10^{-8}$ to be significant.

360 We used a Bayesian approach to identify a set of SNPs with 95% probability of containing the
361 causal variant at the trait-associated locus. Approximate Bayes' factors (*Wakefield, 2009*) were
362 calculated for each SNP in the region (a 200kb surrounding rs183868412) with a prior distribution
363 of $N(0, 0.2^2)$. All SNPs were considered equally likely to be the causal variant a priori. A set of SNPs
364 with 95% probability of containing the causal SNP was defined as the smallest number of SNPs for
365 which the summed posterior probabilities exceed 0.95.

366 **Replication samples and analysis**

367 To replicate our findings from the discovery analysis we used a second sample set, recruited from
368 the same population as the discovery samples. Replication case samples were cases of bacter-
369 aemia only, and did not include cases of severe malaria without culture-confirmed bacterial infec-
370 tion. Case samples were recruited between 1st August 1998 and 30th October 2010. As for the
371 discovery case samples, children under 14 years with a bacterial pathogen isolated from blood on
372 admission to hospital were eligible for recruitment to the study. As above, control samples were
373 recruited as part of a birth cohort from the same population, with children recruited between the
374 ages of 3 and 12 months. Genotyping and QC procedures for these samples have been described
375 previously. In brief, study samples were genotyped using the ImmunoChip Consortium (*Cortes*
376 *and Brown, 2011*) array (Illumina). Sample QC was performed as for the discovery samples (above),
377 with duplicate control samples (samples common to MalariaGEN and ImmunoChip controls, $n=78$)
378 being removed from the replication set. As above, relatedness estimates and PCs were computed
379 in PLINK v1.90 (*Chang et al., 2015*), with the major four PCs of genotype data differentiating self-
380 reported ethnicity (Figure 3-figure supplement 1). SNP QC excluded the following variants; SNP
381 missingness $>1\%$, MAF $<1\%$ and HWE $p < 1 \times 10^{-10}$. Following QC, 143,000 genotyped variants in
382 434 cases and 1,258 control samples were taken forward for imputation. As above, imputation was
383 performed with SHAPEIT2 (*Delaneau et al., 2012*) and IMPUTE2 (v2.3.2) (*Howie et al., 2011, 2009*)
384 with 1000 Genomes Phase III as a reference panel.

385 Following imputation, we further excluded poorly-imputed (imputation info score <0.5) and rare
386 (MAF $<1\%$) variants and variants with HWE $p < 1 \times 10^{-10}$. At variants associated with invasive bacterial
387 disease ($p < 5 \times 10^{-8}$) in the discovery analysis, we tested for association with bacteraemia case-
388 control status using logistic regression in an additive model in SNPTEST v2.5.6 (*Marchini et al.,*
389 *2007*). To exclude confounding variation, we included the major four PCs of genotyping data in the
390 model. We considered evidence of association with bacteraemia in the replication samples with
391 $p < 0.05$ with the same direction of effect as in the discovery analysis to be significant.

392 **Bayesian comparison of models of association**

393 At the locus of interest, we used multinomial logistic regression, implemented in SNPTEST v2.5.6
394 (*Marchini et al., 2007*) to estimate the additive effect of genotype on risk of bacteraemia strati-

395 fied by pathogen, bacteraemia in the neonatal and non-neonatal periods, bacteraemia with and
396 without *P. falciparum* parasitaemia, and bacteraemia presenting at different time periods across a
397 period of declining malaria transmission intensity. For these analyses we used only samples with
398 culture-confirmed bacteraemia. In each case we used control status as the baseline stratum, and
399 included the major principal components of genotyping data to control for confounding variation
400 as above.

401 For the pathogen-stratified analysis, we defined eight case strata among the discovery cases,
402 one for each of the seven most commonly isolated organisms (*Acinetobacter*, n=118; β -haemolytic
403 *Streptococci*, n=130; *E. coli*, n=141; *H. influenzae* type b, n=113; nontyphoidal *Salmonella*, n=159;
404 pneumococci, n=390; *S. aureus*, n=152) and one stratum for the remaining other organisms (n=242).
405 For the neonatal/non-neonatal disease analysis we stratified cases as presenting in the first 28 days
406 of life (n=195) or beyond that (n=1,245). For the analysis comparing bacteraemia with and without
407 malaria we stratified cases with (n=204) and without (n=1,236) *P. falciparum* on their admission
408 blood film. For each of these analysis case strata were compared to Affymetrix-genotyped discov-
409 ery control samples (n=1,895) as a baseline stratum.

410 For the analysis stratified across year of admission, we defined case strata by grouping into six
411 time periods according to their date of admission; 1998-2000 (n=498), 2001-2002 (n=349), 2003-
412 2004 (n=467), 2005-2006 (n=310), 2007-2008 (n=237), 2009-2010 (n=111). For this analysis we used
413 both discovery (Affymetrix) and replication (ImmunoChip) case and control samples. This allowed
414 better coverage of the years later in the study, which were underrepresented in the discovery
415 samples (the discovery median admission year is 2003, c.f. 2005 for the replication samples). In
416 that analysis we used multinomial logistic regression in each cohort to estimate stratum-specific
417 effects, combining these results in a fixed effects meta-analysis using BINGWA (*Band et al., 2015*).

418 We then compared models of association using a Bayesian approach (*Rautanen et al., 2016*),
419 considering the following models:

420 "Null": effect size = i.e. no association with bacteraemia.

421 "Same": effect size $N(0, 0.2^2)$ and fixed across strata.

422 Additional models consider each possible combination of a fixed effect size for associated strata
423 and no association at other strata. For each model we calculated approximate Bayes factors (*Wake-*
424 *field, 2009*) and posterior probabilities, assuming each model to be equally likely a priori. Statistical
425 analysis was performed in R.

426 Co-localisation analysis

427 We used the R package coloc v5.1.0 (*Giambartolomei et al., 2014*) to identify evidence of causal
428 variants shared by our bacterial disease-associated locus of interest and regulatory genetic varia-
429 tion mapped by eQTL studies. We downloaded eQTL summary statistics describing eQTL mapping
430 in naive and stimulated monocytes (*Quach et al., 2016*), including study participants with African an-
431 cestry, from the eQTL catalogue (*Kerimov et al., 2021*) (<https://github.com/eQTL-Catalogue/eQTL-Catalogue-res>
432 accessed 28th October 2021). Coloc adopts a Bayesian approach to compare evidence for indepen-
433 dent or shared association signals for two traits at a given genetic locus. We used the coloc.susie()
434 command to allow co-localisation of multiple independent signals at a single locus for each trait.
435 We tested for colocalisation between invasive bacterial disease susceptibility at the *BIRC6* locus
436 and previously-published eQTL data in naive and stimulated primary monocytes isolated from in-
437 dividuals of European (n=100) and African (n=100) ancestry (*Quach et al., 2016*). We considered
438 evidence for co-localisation for each gene and exon within a 250kb window of the peak associa-
439 tion (rs183868412). We considered a posterior probability > 0.8 supporting a shared causal locus
440 to be significant.

441 Acknowledgments

442 This publication uses genotyping data from the MalariaGEN consortial project, as described in
443 Malaria Genomic Epidemiology Network, et al. Nature Communications, 2019 (<https://doi.org/10.1038/s41467-019-14444-4>)

444 019-13480-z). This study makes use of data generated by the Wellcome Trust Case Control Consor-
445 tium 2 project (Grant Reference 085475/B/08/Z). JJG and AJM are funded by National Institute for
446 Health Research (NIHR) Clinical Lectureships. TNW and JAGS are supported by Senior Research Fel-
447 lowships from the Wellcome Trust (202800 and 098532 respectively). JAW is a Sir Henry Dale Fellow
448 funded by the Wellcome Trust (223253/Z/21/Z). SMAART (Severe Malaria Africa – A consortium for
449 Research and Trials) is funded by a Wellcome Collaborative Award in Science grant (209265/Z/17/Z)
450 held in part by KM and TNW. During this work AVSH was supported by a Wellcome Trust Senior
451 Investigator Award (HCUZZ0) and by a European Research Council advanced grant (294557). The
452 research was supported by the Wellcome Trust Core Award Grant Number 203141/Z/16/Z with
453 additional support from the NIHR Oxford BRC. The views expressed are those of the author(s) and
454 not necessarily those of the NHS, the NIHR or the Department of Health. This research was funded
455 by The Wellcome Trust. A CC BY or equivalent licence is applied to the author accepted manuscript
456 arising from this submission, in accordance with the grant's open access conditions. This paper is
457 published with the permission of the Director of KEMRI.

458 References

- 459 **Albert ML.** Death-defying immunity: do apoptotic cells influence antigen processing and presentation? *Nature*
460 *Reviews Immunology*. 2004; 4(3):223–231. <https://doi.org/10.1038/nri11308>, doi: 10.1038/nri11308.
- 461 **Band G,** Le QS, Clarke GM, Kivinen K, Hubbart C, Jeffreys AE, Rowlands K, Leffler EM, Jallow M, Conway DJ, Sisay-
462 Joof F, Sirugo G, d'Alessandro U, Toure OB, Thera MA, Konate S, Sissoko S, Mangano VD, Bougouma EC, Sirima
463 SB, et al. Insights into malaria susceptibility using genome-wide data on 17,000 individuals from Africa, Asia
464 and Oceania. *Nature Communications*. 2019; 10(1):5732. <https://doi.org/10.1038/s41467-019-13480-z>, doi:
465 10.1038/s41467-019-13480-z.
- 466 **Band G,** Rockett KA, Spencer CCA, Kwiatkowski DP, Si Le Q, Clarke GM, Kivinen K, Leffler EM, Rockett KA,
467 Kwiatkowski DP, Spencer CCA, Rockett KA, Spencer CCA, Cornelius V, Conway DJ, Williams TN, Taylor T,
468 Kwiatkowski DP, Conway DJ, Bojang KA, et al. A novel locus of resistance to severe malaria in a region of
469 ancient balancing selection. *Nature*. 2015; 526(7572):253–257. <https://doi.org/10.1038/nature15390>, doi:
470 10.1038/nature15390.
- 471 **Bartke T,** Pohl C, Pyrowolakis G, Jentsch S. Dual Role of BRUCE as an Antiapoptotic IAP and a Chimeric E2/E3
472 Ubiquitin Ligase. *Molecular Cell*. 2004; 14(6):801–811. [https://www.sciencedirect.com/science/article/pii/](https://www.sciencedirect.com/science/article/pii/S1097276504003041)
473 [S1097276504003041](https://doi.org/10.1016/j.molcel.2004.05.018), doi: <https://doi.org/10.1016/j.molcel.2004.05.018>.
- 474 **Bejon P,** Berkley JA, Mwangi T, Ogada E, Mwangi I, Maitland K, Williams T, Scott JAG, English M, Lowe BS, Peshu
475 N, Newton CRJC, Marsh K. Defining childhood severe falciparum malaria for intervention studies. *PLoS Med*.
476 2007 Aug; 4(8):e251. doi: 10.1371/journal.pmed.0040251.
- 477 **Berkley JA,** Lowe BS, Mwangi I, Williams T, Bauni E, Mwarumba S, Ngetsa C, Slack MPE, Njenga S, Hart CA,
478 Maitland K, English M, Marsh K, Scott JAG. Bacteremia among children admitted to a rural hospital in Kenya.
479 *N Engl J Med*. 2005 Jan; 352(1):39–47. doi: 10.1056/NEJMoa040275.
- 480 **Bustamante J,** Boisson-Dupuis S, Abel L, Casanova JL. Mendelian susceptibility to mycobacterial disease: ge-
481 netic, immunological, and clinical features of inborn errors of IFN- immunity. *Semin Immunol*. 2014 Dec;
482 26(6):454–470. doi: 10.1016/j.smim.2014.09.008.
- 483 **Chang CC,** Chow CC, Tellier LC, Vattikuti S, Purcell SM, Lee JJ. Second-generation PLINK: rising to the challenge
484 of larger and richer datasets. *Gigascience*. 2015; 4:7. doi: 10.1186/s13742-015-0047-8.
- 485 **Church J,** Maitland K. Invasive bacterial co-infection in African children with Plasmodium falciparum malaria:
486 a systematic review. *BMC Med*. 2014 Feb; 12:31. doi: 10.1186/1741-7015-12-31.
- 487 **Cortes A,** Brown MA. Promise and pitfalls of the Immunochip. *Arthritis Res Ther*. 2011 Feb; 13(1):101. doi:
488 10.1186/ar3204.
- 489 **Cowgill KD,** Ndiritu M, Nyiro J, Slack MPE, Chipshatsi S, Ismail A, Kamau T, Mwangi I, English M, Newton CRJC,
490 Feikin DR, Scott JAG. Effectiveness of Haemophilus influenzae Type b Conjugate Vaccine Introduction Into
491 Routine Childhood Immunization in Kenya. *JAMA*. 2006 11/3/2021; 296(6):671–678. [https://doi.org/10.1001/](https://doi.org/10.1001/jama.296.6.671)
492 [jama.296.6.671](https://doi.org/10.1001/jama.296.6.671), doi: 10.1001/jama.296.6.671.

- 493 **Davila S**, Wright VJ, Khor CC, Sim KS, Binder A, Breunis WB, Inwald D, Nadel S, Betts H, Carrol ED, de Groot
494 R, Hermans PWM, Hazelzet J, Emonts M, Lim CC, Kuijpers TW, Martinon-Torres F, Salas A, Zenz W, Levin M,
495 et al. Genome-wide association study identifies variants in the CFH region associated with host susceptibil-
496 ity to meningococcal disease. *Nature Genetics*. 2010; 42(9):772–776. <https://doi.org/10.1038/ng.640>, doi:
497 [10.1038/ng.640](https://doi.org/10.1038/ng.640).
- 498 **Delaneau O**, Marchini J, Zagury JF. A linear complexity phasing method for thousands of genomes. *Nature*
499 *Methods*. 2012; 9(2):179–181. <https://doi.org/10.1038/nmeth.1785>, doi: [10.1038/nmeth.1785](https://doi.org/10.1038/nmeth.1785).
- 500 **Deretic V**, Saitoh T, Akira S. Autophagy in infection, inflammation and immunity. *Nature Reviews Immunology*.
501 2013; 13(10):722–737. <https://doi.org/10.1038/nri3532>, doi: [10.1038/nri3532](https://doi.org/10.1038/nri3532).
- 502 **Driscoll AJ**, Deloria Knoll M, Hammitt LL, Baggett HC, Brooks WA, Feikin DR, Kotloff KL, Levine OS, Madhi SA,
503 O'Brien KL, Scott JAG, Thea DM, Howie SRC, Adrian PV, Ahmed D, DeLuca AN, Ebruke BE, Gitahi C, Higdon
504 MM, Kaewpan A, et al. The Effect of Antibiotic Exposure and Specimen Volume on the Detection of Bacterial
505 Pathogens in Children With Pneumonia. *Clinical Infectious Diseases*. 2017 11/16/2021; 64(suppl_3):S368–
506 S377. <https://doi.org/10.1093/cid/cix101>, doi: [10.1093/cid/cix101](https://doi.org/10.1093/cid/cix101).
- 507 **Ebner P**, Poetsch I, Deszcz L, Hoffmann T, Zuber J, Ikeda F. The IAP family member BRUCE regulates
508 autophagosome-lysosome fusion. *Nat Commun*. 2018 Feb; 9(1):599. doi: [10.1038/s41467-018-02823-x](https://doi.org/10.1038/s41467-018-02823-x).
- 509 **Figueroa J**, Andreoni J, Densen P. Complement deficiency states and meningococcal disease. *Immunol Res*.
510 1993; 12(3):295–311. doi: [10.1007/BF02918259](https://doi.org/10.1007/BF02918259).
- 511 **Giambartolomei C**, Vukcevic D, Schadt EE, Franke L, Hingorani AD, Wallace C, Plagnol V. Bayesian test for
512 colocalisation between pairs of genetic association studies using summary statistics. *PLoS Genet*. 2014 May;
513 10(5):e1004383. doi: [10.1371/journal.pgen.1004383](https://doi.org/10.1371/journal.pgen.1004383).
- 514 **Gilchrist JJ**, Rautanen A, Fairfax BP, Mills TC, Naranbhai V, Trochet H, Pirinen M, Muthumbi E, Mwarumba S,
515 Njuguna P, Mturi N, Msefula CL, Gondwe EN, MacLennan JM, Chapman SJ, Molyneux ME, Knight JC, Spencer
516 CCA, Williams TN, MacLennan CA, et al. Risk of nontyphoidal Salmonella bacteraemia in African children is
517 modified by STAT4. *Nature Communications*. 2018; 9(1):1014. <https://doi.org/10.1038/s41467-017-02398-z>,
518 doi: [10.1038/s41467-017-02398-z](https://doi.org/10.1038/s41467-017-02398-z).
- 519 **Hao Y**, Sekine K, Kawabata A, Nakamura H, Ishioka T, Ohata H, Katayama R, Hashimoto C, Zhang X, Noda T,
520 Tsuruo T, Naito M. Apollon ubiquitinates SMAC and caspase-9, and has an essential cytoprotection function.
521 *Nature Cell Biology*. 2004; 6(9):849–860. <https://doi.org/10.1038/ncb1159>, doi: [10.1038/ncb1159](https://doi.org/10.1038/ncb1159).
- 522 **Hauser HP**, Bardroff M, Pyrowolakis G, Jentsch S. A giant ubiquitin-conjugating enzyme related to IAP apoptosis
523 inhibitors. *J Cell Biol*. 1998 Jun; 141(6):1415–1422. doi: [10.1083/jcb.141.6.1415](https://doi.org/10.1083/jcb.141.6.1415).
- 524 **Hendriksen ICE**, Mwanga-Amumpaire J, von Seidlein L, Mtove G, White LJ, Olaosebikan R, Lee SJ, Tshefu AK,
525 Woodrow C, Amos B, Karema C, Saiwaew S, Maitland K, Gomes E, Pan-Ngum W, Gesase S, Silamut K, Reyburn
526 H, Joseph S, Chotivanich K, et al. Diagnosing severe falciparum malaria in parasitaemic African children: a
527 prospective evaluation of plasma PfHRP2 measurement. *PLoS Med*. 2012; 9(8):e1001297. doi: [10.1371/jour-
528 nal.pmed.1001297](https://doi.org/10.1371/journal.pmed.1001297).
- 529 **Hoogerwerf JJ**, van Zoelen MA, Wiersinga WJ, van 't Veer C, de Vos AF, de Boer A, Schultz MJ, Hooibrink B,
530 de Jonge E, van der Poll T. Gene expression profiling of apoptosis regulators in patients with sepsis. *J Innate*
531 *Immun*. 2010; 2(5):461–468. doi: [10.1159/000317035](https://doi.org/10.1159/000317035).
- 532 **Hotchkiss RS**, Tinsley KW, Swanson PE, Schmiege REJ, Hui JJ, Chang KC, Osborne DF, Freeman BD, Cobb JP, Buch-
533 man TG, Karl IE. Sepsis-induced apoptosis causes progressive profound depletion of B and CD4+ T lympho-
534 cytes in humans. *J Immunol*. 2001 Jun; 166(11):6952–6963. doi: [10.4049/jimmunol.166.11.6952](https://doi.org/10.4049/jimmunol.166.11.6952).
- 535 **Hotchkiss RS**, Nicholson DW. Apoptosis and caspases regulate death and inflammation in sepsis. *Nat Rev*
536 *Immunol*. 2006 Nov; 6(11):813–822. doi: [10.1038/nri1943](https://doi.org/10.1038/nri1943).
- 537 **Hotchkiss RS**, Tinsley KW, Swanson PE, Grayson MH, Osborne DF, Wagner TH, Cobb JP, Coopersmith C, Karl IE.
538 Depletion of dendritic cells, but not macrophages, in patients with sepsis. *J Immunol*. 2002 Mar; 168(5):2493–
539 2500. doi: [10.4049/jimmunol.168.5.2493](https://doi.org/10.4049/jimmunol.168.5.2493).
- 540 **Howie B**, Marchini J, Stephens M. Genotype imputation with thousands of genomes. *G3 (Bethesda)*. 2011 Nov;
541 1(6):457–470. doi: [10.1534/g3.111.001198](https://doi.org/10.1534/g3.111.001198).

- 542 **Howie BN**, Donnelly P, Marchini J. A flexible and accurate genotype imputation method for the next gen-
543 eration of genome-wide association studies. *PLoS Genet.* 2009 Jun; 5(6):e1000529. doi: [10.1371/jour-](https://doi.org/10.1371/journal.pgen.1000529)
544 [nal.pgen.1000529](https://doi.org/10.1371/journal.pgen.1000529).
- 545 **Jia R**, Bonifacino JS. Negative regulation of autophagy by UBA6-BIRC6-mediated ubiquitination of LC3. *Elife.*
546 2019 Nov; 8. doi: [10.7554/eLife.50034](https://doi.org/10.7554/eLife.50034).
- 547 **Kerimov N**, Hayhurst JD, Peikova K, Manning JR, Walter P, Kolberg L, Samoviča M, Sakthivel MP, Kuzmin I, Tre-
548 vanion SJ, Burdett T, Jupp S, Parkinson H, Papatheodorou I, Yates AD, Zerbino DR, Alasoo K. A compendium
549 of uniformly processed human gene expression and splicing quantitative trait loci. *Nature Genetics.* 2021;
550 53(9):1290–1299. <https://doi.org/10.1038/s41588-021-00924-w>, doi: 10.1038/s41588-021-00924-w.
- 551 **Le Tulzo Y**, Pangault C, Gacouin A, Guilloux V, Tribut O, Amiot L, Tattevin P, Thomas R, Fauchet R, Drénou B.
552 Early circulating lymphocyte apoptosis in human septic shock is associated with poor outcome. *Shock.* 2002
553 Dec; 18(6):487–494. doi: 10.1097/00024382-200212000-00001.
- 554 **Lo S**, Yuan SSF, Hsu C, Cheng YJ, Chang YF, Hsueh HW, Lee PH, Hsieh YC. Lc3 Over-Expression Improves Survival
555 and Attenuates Lung Injury Through Increasing Autophagosomal Clearance in Septic Mice. *Annals of Surgery.*
556 2013; 257(2). [https://journals.lww.com/annalsurgery/Fulltext/2013/02000/Lc3_Over_Expression_Improves_](https://journals.lww.com/annalsurgery/Fulltext/2013/02000/Lc3_Over_Expression_Improves_Survival_and.26.aspx)
557 [Survival_and.26.aspx](https://journals.lww.com/annalsurgery/Fulltext/2013/02000/Lc3_Over_Expression_Improves_Survival_and.26.aspx).
- 558 **Marchini J**, Howie B, Myers S, McVean G, Donnelly P. A new multipoint method for genome-wide association
559 studies by imputation of genotypes. *Nature Genetics.* 2007; 39(7):906–913. <https://doi.org/10.1038/ng2088>,
560 doi: 10.1038/ng2088.
- 561 **Ndila CM**, Uyoga S, Macharia AW, Nyutu G, Peshu N, Ojal J, Shebe M, Awuondo KO, Mturi N, Tsofa B, Sepúlveda
562 N, Clark TG, Band G, Clarke G, Rowlands K, Hubbart C, Jeffreys A, Kariuki S, Marsh K, Mackinnon M, et al.
563 Human candidate gene polymorphisms and risk of severe malaria in children in Kilifi, Kenya: a case-control
564 association study. *Lancet Haematol.* 2018 Aug; 5(8):e333–e345. doi: 10.1016/S2352-3026(18)30107-8.
- 565 **Picard C**, von Bernuth H, Ku CL, Yang K, Puel A, Casanova JL. Inherited human IRAK-4 deficiency: an update.
566 *Immunol Res.* 2007; 38(1-3):347–352. doi: 10.1007/s12026-007-0006-2.
- 567 **Quach H**, Rotival M, Pothlichet J, Loh YHE, Dannemann M, Zidane N, Laval G, Patin E, Harmant C, Lopez M,
568 Deschamps M, Naffakh N, Duffy D, Coen A, Leroux-Roels G, Clément F, Boland A, Deleuze JF, Kelso J, Albert
569 ML, et al. Genetic Adaptation and Neandertal Admixture Shaped the Immune System of Human Populations.
570 *Cell.* 2016 Oct; 167(3):643–656. doi: [10.1016/j.cell.2016.09.024](https://doi.org/10.1016/j.cell.2016.09.024).
- 571 **Rautanen A**, Pirinen M, Mills TC, Rockett KA, Strange A, Ndungu AW, Naranbhai V, Gilchrist JJ, Bellenguez C,
572 Freeman C, Band G, Bumpstead SJ, Edkins S, Giannoulatou E, Gray E, Dronov S, Hunt SE, Langford C, Pearson
573 RD, Su Z, et al. Polymorphism in a lincRNA Associates with a Doubled Risk of Pneumococcal Bacteremia in
574 Kenyan Children. *Am J Hum Genet.* 2016 Jun; 98(6):1092–1100. doi: [10.1016/j.ajhg.2016.03.025](https://doi.org/10.1016/j.ajhg.2016.03.025).
- 575 **Scott JAG**, Berkley JA, Mwangi I, Ochola L, Uyoga S, Macharia A, Ndila C, Lowe BS, Mwarumba S, Bauni E, Marsh K,
576 Williams TN. Relation between falciparum malaria and bacteraemia in Kenyan children: a population-based,
577 case-control study and a longitudinal study. *Lancet.* 2011 Oct; 378(9799):1316–1323. doi: 10.1016/S0140-
578 6736(11)60888-X.
- 579 **Silaba M**, Ooko M, Bottomley C, Sande J, Benamore R, Park K, Ignas J, Maitland K, Mturi N, Makumi A, Otiende
580 M, Kagwanja S, Safari S, Ochola V, Bwanaali T, Bauni E, Gleeson F, Deloria Knoll M, Adetifa I, Marsh K,
581 et al. Effect of 10-valent pneumococcal conjugate vaccine on the incidence of radiologically-confirmed
582 pneumonia and clinically-defined pneumonia in Kenyan children: an interrupted time-series analysis. *The*
583 *Lancet Global Health.* 2019 2021/11/03; 7(3):e337–e346. [https://doi.org/10.1016/S2214-109X\(18\)30491-1](https://doi.org/10.1016/S2214-109X(18)30491-1),
584 doi: 10.1016/S2214-109X(18)30491-1.
- 585 **Verhagen AM**, Coulson EJ, Vaux DL. Inhibitor of apoptosis proteins and their relatives: IAPs and other
586 BIRPs. *Genome Biology.* 2001; 2(7):reviews3009.1. <https://doi.org/10.1186/gb-2001-2-7-reviews3009>, doi:
587 10.1186/gb-2001-2-7-reviews3009.
- 588 **Vos T**, Lim SS, Abbafati C, Abbas KM, Abbasi M, Abbasifard M, Abbasi-Kangevari M, Abbastabar H, Abd-Allah
589 F, Abdelalim A, Abdollahi M, Abdollahpour I, Abolhassani H, Aboyans V, Abrams EM, Abreu LG, Abrigo MRM,
590 Abu-Raddad LJ, Abushouk AI, Acebedo A, et al. Global burden of 369 diseases and injuries in 204 coun-
591 tries and territories, 1990–2013; 2019: a systematic analysis for the Global Burden of Disease Study 2019.
592 *The Lancet.* 2020 2021/11/03; 396(10258):1204–1222. [https://doi.org/10.1016/S0140-6736\(20\)30925-9](https://doi.org/10.1016/S0140-6736(20)30925-9), doi:
593 10.1016/S0140-6736(20)30925-9.

- 594 **Wakefield J.** Bayes factors for genome-wide association studies: comparison with P-values. *Genet Epidemiol.*
595 2009 Jan; 33(1):79–86. doi: [10.1002/gepi.20359](https://doi.org/10.1002/gepi.20359).
- 596 **Watson JA,** Ndila CM, Uyoga S, Macharia A, Nyutu G, Mohammed S, Ngetsu C, Mturi N, Peshu N, Tsofa B, Rockett
597 K, Leopold S, Kingston H, George EC, Maitland K, Day NP, Dondorp AM, Bejon P, Williams T, Holmes CC,
598 et al. Improving statistical power in severe malaria genetic association studies by augmenting phenotypic
599 precision. *Elife.* 2021 Jul; 10. doi: [10.7554/eLife.69698](https://doi.org/10.7554/eLife.69698).
- 600 **Watson JA,** Uyoga S, Wanjiku P, Makale J, Nyutu GM, Mturi N, George EC, Woodrow CJ, Day NP, Bejon P, Opoka
601 RO, Dondorp AM, John CC, Maitland K, Williams TN, White NJ. Improving the diagnosis of severe malaria
602 in African children using platelet counts and plasma Pf HRP2 concentrations. *medRxiv.* 2021; [https://www.](https://www.medrxiv.org/content/early/2021/10/30/2021.10.27.21265557)
603 [medrxiv.org/content/early/2021/10/30/2021.10.27.21265557](https://www.medrxiv.org/content/early/2021/10/30/2021.10.27.21265557), doi: [10.1101/2021.10.27.21265557](https://doi.org/10.1101/2021.10.27.21265557).
- 604 **Williams TN,** Uyoga S, Macharia A, Ndila C, McAuley CF, Opi DH, Mwarumba S, Makani J, Komba A, Ndiritu
605 MN, Sharif SK, Marsh K, Berkley JA, Scott JAG. Bacteraemia in Kenyan children with sickle-cell anaemia: a
606 retrospective cohort and case-control study. *Lancet.* 2009 Oct; 374(9698):1364–1370. doi: [10.1016/S0140-](https://doi.org/10.1016/S0140-6736(09)61374-X)
607 [6736\(09\)61374-X](https://doi.org/10.1016/S0140-6736(09)61374-X).

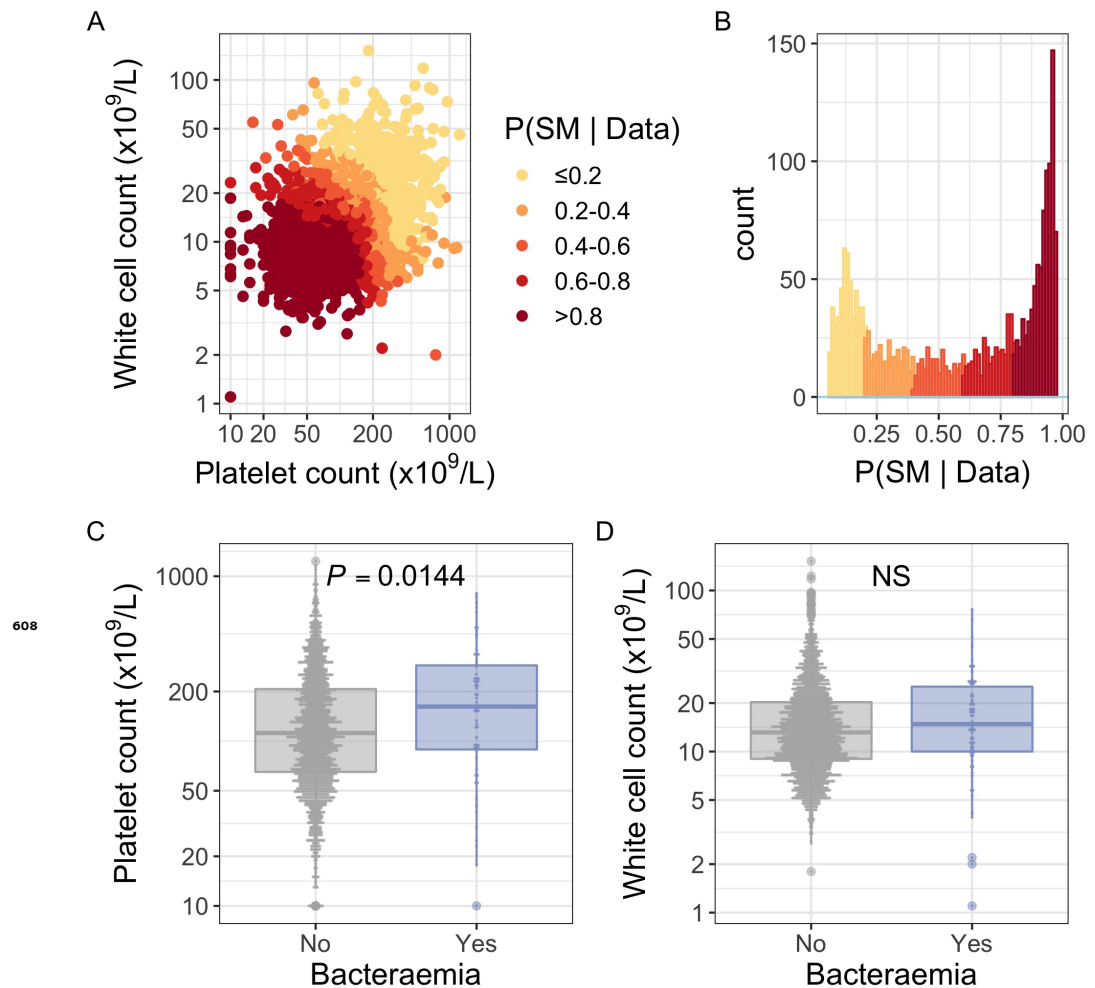


Figure 1-Figure supplement 1. White blood cell and platelet count as predictors of severe malaria. (A) Distribution of white blood cell and platelet count among Kenyan children ($n=2,200$) with a clinical diagnosis of severe malaria. Points are coloured according to the probability of 'true' severe malaria given the data. (B) Distribution of 'true' severe malaria probabilities estimated from platelet count and white blood cell count. (C) Platelets counts in children with a clinical diagnosis of severe malaria with and without concomitant bacteraemia. (D) White blood cell counts in children with a clinical diagnosis of severe malaria with and without concomitant bacteraemia.

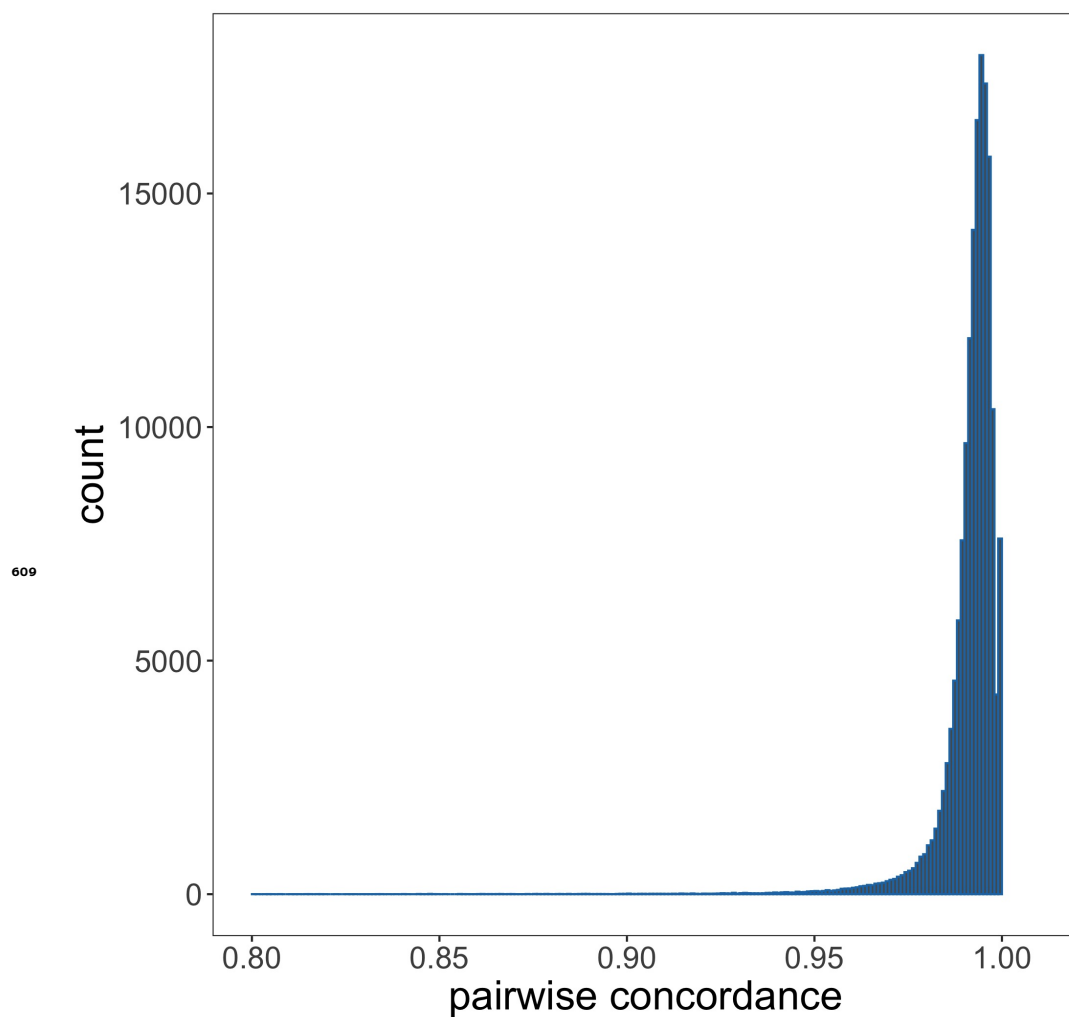


Figure 2-Figure supplement 1. Genotyping concordance between Illumina and Affymetrix platforms. Pairwise genotyping concordance between samples genotyped on both Affymetrix SNP 6.0 and Illumina Omni 2.5M platforms.

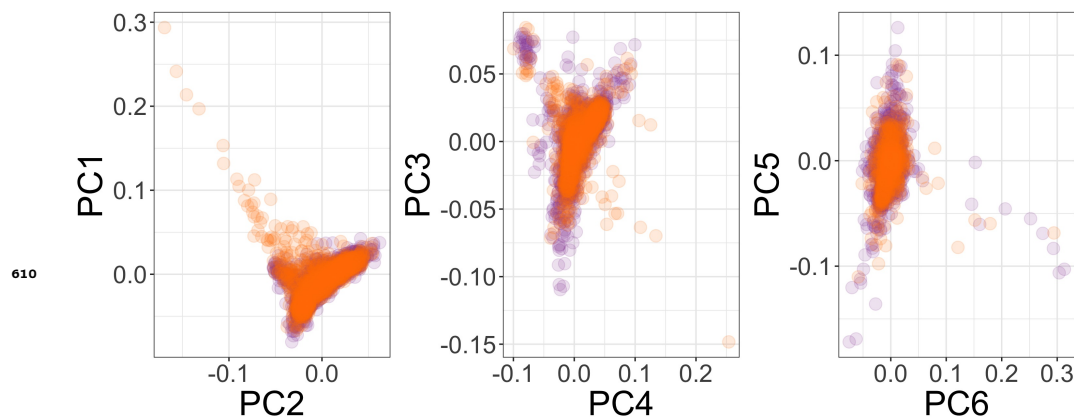


Figure 2-Figure supplement 2. Principal components of genome-wide genotyping data in discovery samples. Individuals are color-coded according to genotyping platform; Affymetrix SNP 6.0 in purple, Illumina Omni 2.5M in orange.

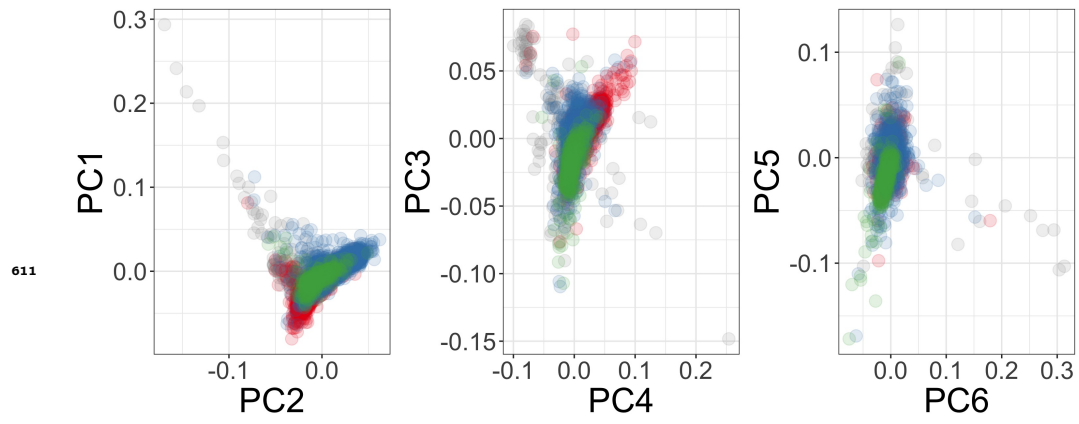


Figure 2-Figure supplement 3. Principal components of genome-wide genotyping data in discovery samples. Individuals are color-coded according to self-reported ethnicity; Chonyi in red, Giriama in blue, Kauma in green and other in grey.

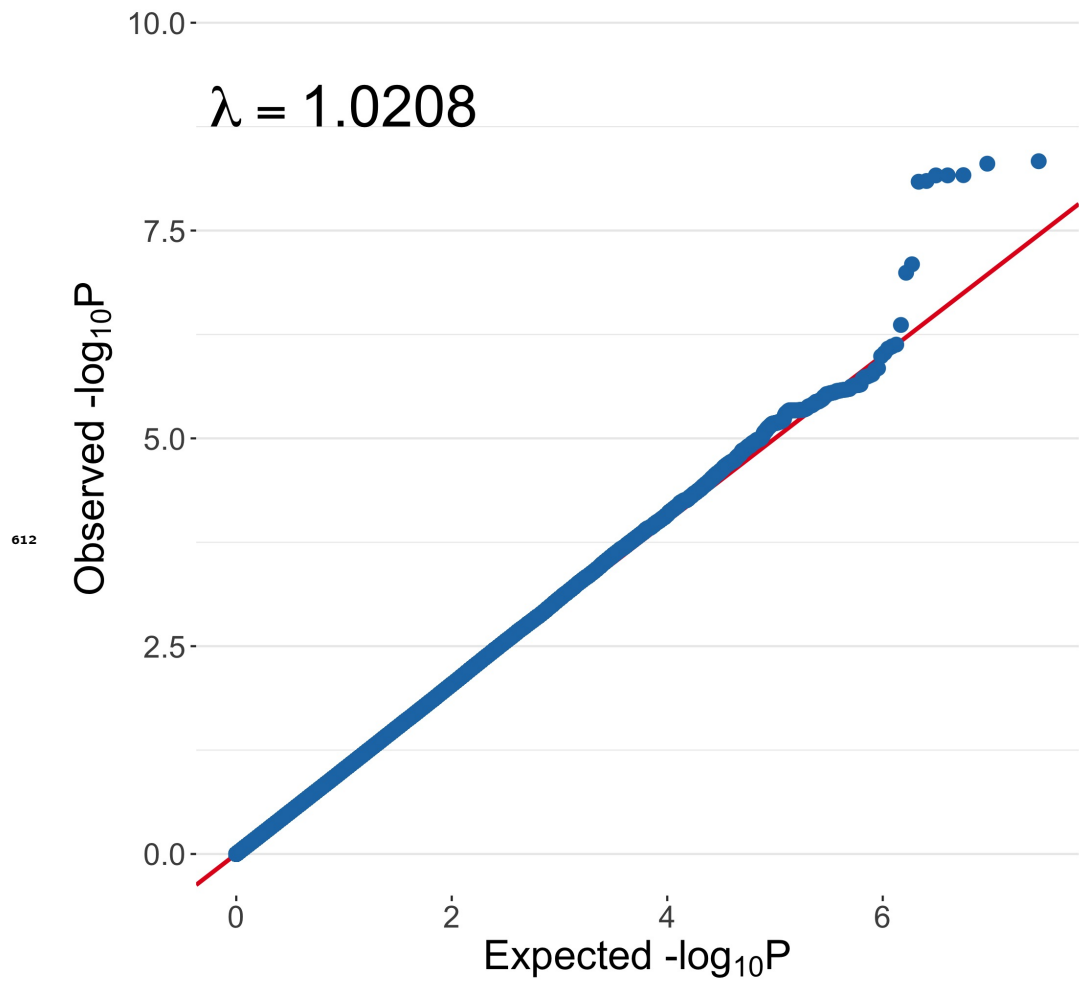


Figure 2-Figure supplement 4. Quantile-quantile plot of invasive bacterial infection in Kenyan children. QQ plot of weighted logistic regression GWAS of invasive bacterial disease in Kenyan children (2,588 cases, 2,812 controls).

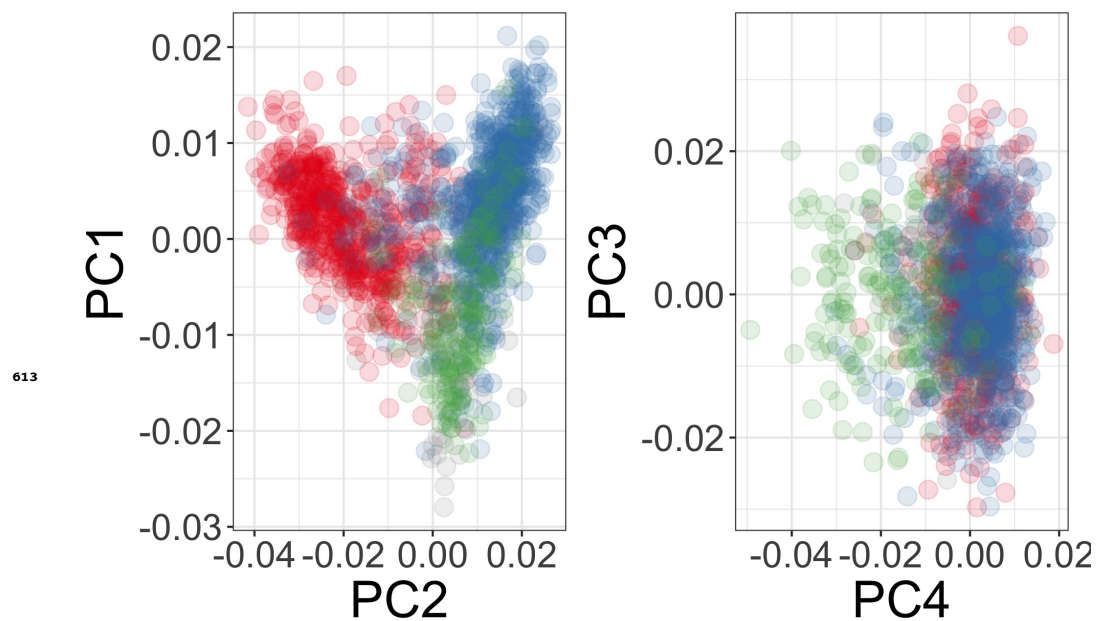


Figure 3-Figure supplement 1. Principal components of genome-wide genotyping data in replication samples. Individuals are color-coded according to self-reported ethnicity; Chonyi in red, Giriama in blue, Kauma in green and other in grey.